DEUTSCHES ELEKTRONEN-SYNCHROTRON DESY

DESY 85-073
July 1985

RECENT MEASUREMENTS OF TWO PHOTON MUON PAIR PROCESS FROM MARK J AT $\sqrt{s}$ UP TO 46.78 GEV

MARK J Collaboration

ISSN 0418-9833

NOTKESTRASSE 85 · 2 HAMBURG 52

To be sure that your preprints are promptly included in the
HIGH ENERGY PHYSICS INDEX ,
send them to the following address (if possible by air mail) :

DESY
Bibliothek
Notkestrasse 85
2 Hamburg 52
Germany

DESY 85-073
July 1985

ISSN 0418-9833

RECENT MEASUREMENTS OF TWO PHOTON MUON PAIR PROCESS FROM MARK J

AT $\sqrt{s}$ UPTO 46.78 GEV

The Mark J Collaboration

presented by C.C.Zhang*

ABSTRACT

The recent results from Mark J on two photon muon pair production with $\sqrt{s}$ from 14 to 46.78 GeV are presented, and compared with the complete α^4 QED calculation in a large range of $\sqrt{s}$ and four momentum transfer, including untagged, single and double tagged events. The forward-backward charge asymmetry of muons produced in the two photon process is also compared to the QED prediction.

*A talk at the workshop on the test of Electroweak Theory in Trieste, Italy.

1 INTRODUCTION

The test of QED to α^4 using two photon process

$$e^+e^- \rightarrow e^+e^-\mu^+\mu^- \qquad (1)$$

at $\sqrt{s}$ = 35 GeV has been reported previously.[1),2),3)] A study of this process at higher energies is interesting for the following reasons:

1. To test QED at large values of $M\mu\mu$, Q^2 and P_t.
   PETRA has reached highest energy of $\sqrt{s}$ = 46.78 GeV and a large integrated luminosity has been collected in the range $\sqrt{s} \geq 40$ GeV. This makes it possible to test QED to α^4 in the large invariant mass of muon pairs, large transverse momentum of muons and large Q^2, four momentum transfer, between incoming and outgoing electrons.
   Higher statistics data with single and double tagged events can be compared with a newly complete α^4 QED Monte Carlo calculation.

2. Searching for new particles.
   The process of $e^+e^- \rightarrow e^+e^-\mu^+\mu^-$ can be well measured experimently and precisely calculated by QED theory. An excess above the QED prediction would be an indication of new particle production, e.g. a new state X with charge parity C = +1 could show up as a peak in the distribution of invariant mass of muon pair via $\gamma\gamma$ collisions :

   $$\gamma\gamma \rightarrow X \rightarrow l^+l^-. \qquad (2)$$

3. The two photon muon pair production can be seen as a prototype reaction for quark pair production in the two photon process. A good measurement of the $ee\mu\mu$ final state would give us the basic information for $eeq\bar{q}$ studies[4)].

We report the new $ee\mu\mu$ analysis by the Mark J experiment at $\sqrt{s} \leq 46.78$ GeV. The results of single and double tagged events with averaged Q^2 = 44 and 166 GeV^2 are also presented. So is the charge asymmetry of muons.

2 DATA COLLECTION AND EVENT SELECTION

1. Mark J detector.

   Details of the Mark J detector can be found in ref. 5. The following gives a brief desription of these parts of the detector most relevant to the measurement of the $ee\mu\mu$ final state.

a. Vertex detector

The vertex detector consists of 2616 drift tubes which are arranged in four rectangular layers surrounding the beam pipe. The resolution per tube is about 0.3 mm. Tracks are reconstructed using $\geq$ 4 tube hits. Charged and neutral particles can be distinguished. The polar angle of charged particle (e.g. e, μ, h) emerging from the interaction region is measured from the drift tube hits.

b. The calorimeters

The electromagnetic calorimeter is subdivided into three layers (A, B and C) of counters, 3, 3 and 12 radiation lengths thick, respectively. It covers an angular region from ϑ = 12° to 168°. The z positions of particle trajectories along the beam direction measured by the electromagnetic calorimeter was found to be in good agreement with that from drift tube tracks. The energy resolution of the calorimeter is 7% at $\sqrt{s}$ = 34 GeV.

c. Muon spectrometer

Muons penetrating the calorimeter go through the 12 planes of inner drift chambers(S,T) and 10(or 12) planes of large area outer drift chambers(P,R). Both end cap regions are covered by an additional 10 planes of end cap drift chambers(U,V). The toroidal iron magnet is installed between inner and outer chambers, which provides a minimum bending power of 1.7 Tesla.m and a minimum total material thickness of 5.4 hadronic interaction lengths to filter out hadrons. Muons are identified by their ability to penetrate the magnet iron.

The fractional errors in inverse momentum for muons from the ee $\rightarrow \mu\mu$ reaction with Acol < 5 ° (see eq.(7)). are shown in Table 1 and Fig. 1 . The error contribution from multiple Coulomb scatterring is inversely proportional to P_μ. P_μ is the muon momentum. The muon bending angle in the magnetic field is also inversely proportional to P_μ. The errors in Table 1. show that at low momentem the fractional error in inverse momentum is about 22%, and there is an additional error in the bending angle determination due to the drift chamber for high momentum muons.

Table 1.

The momentum resolution of the Mark J detector for different values of muon momentum from the reaction ee $\rightarrow \mu\mu$, with Acol < 5°. The resolution for the invariant mass of the muon pair is also shown.

P_μ	7 GeV	11 GeV	17.5 GeV
$\Delta(1/P_\mu)/(1/P_\mu)$	22%	28%	32%
$\Delta M_{\mu\mu}/M_{\mu\mu}$	15%	23%	26%

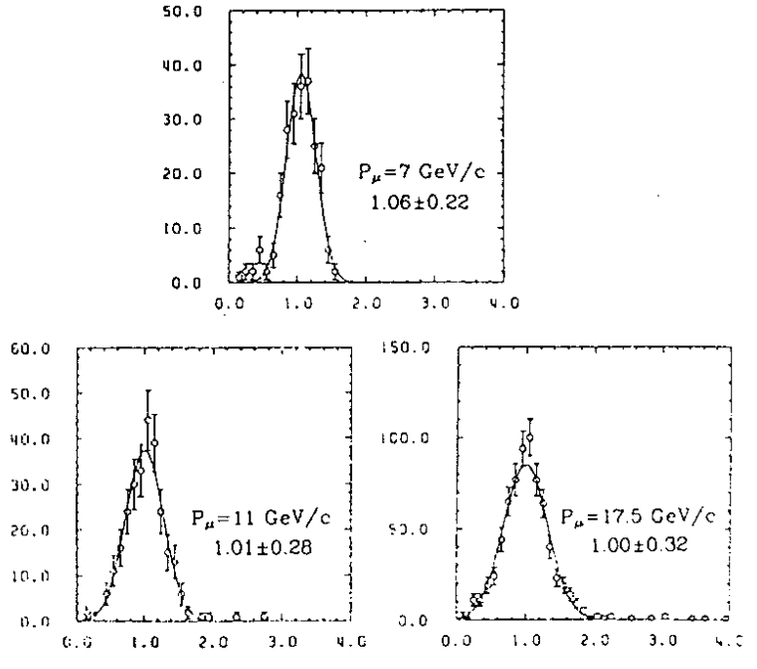

Fig. 1 E_{beam}/P_μ for each muon ploted for P_μ = 7, 11, 17.5 GeV/c separately.

d. The time of flight counter

The 32 TOF counters (D) are sandwiched halfway through the magnetic yoke to trigger on muons and to reject cosmic rays. The time resolution of the counter is 0.6 ns. The separation of di-muon events from cosmic rays using TOF is shown in Fig. 2 .

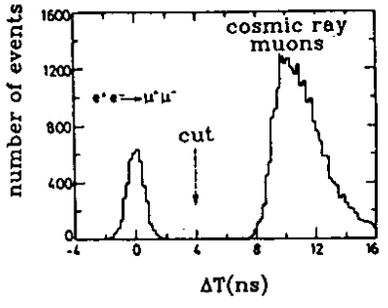

Fig. 2 The distribution of measured time differences between two muon trigger counters.

2. Selection criteria for ee $\to$ ee$\mu\mu$

Events from the reaction of ee $\to$ ee$\mu\mu$ observed in the Mark J detector contain two minimum ionizing tracks with and without additional energetic electromagnetic showers. Muons with large momentum will go through the inner chambers, penetrate about 100 cm of magnetized iron, hit TOF counters and reach the outer chambers, while muons with low momentum may stop in the calorimeter or magnetic iron. The muons for the ee $\to$ ee$\mu\mu$ are identified by reconstructable tracks in the inner chambers and the trigger TOF counters.

In addition, to reject cosmic ray muons the following criteria are imposed for selected events:

a). both muons emerge from within a region of ±5 cm along the beam direction centered at the beam interaction point.

b). the time coincidence of the TOF counter with the beam gate is within 5 nsec.

c). the time difference $\Delta T = T_{bot} - T_{top}$ between the TOF counters hit by each muon must be less than 4 nsec.

To distinguish two photon muons from one photon muons, we use the fact that the momentum spectrum of muons from the one photon process peak at beam energy while the muons produced in the two photon interactions have much lower momentum (see Fig. 3). They can be clearly seperated using a momentum cut.

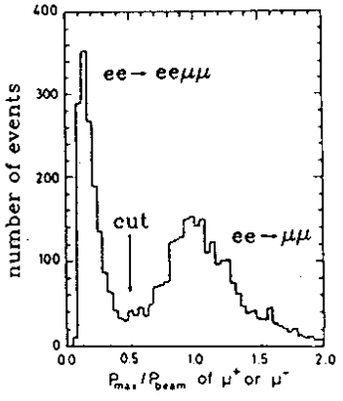

Fig. 3 The distribution of maximum momentum showing how the cut separates ee$\mu\mu$ from $\mu\mu$.

All the selected ee$\mu\mu$ events have been scanned with interactive programs at graphical terminals. One can view the event in several projections and perform track fitting.

The ee$\mu\mu$ events detected can be classified in three categories, with final state particles $\mu\mu$, e$\mu\mu$, or ee$\mu\mu$ observed. The selection criteria for the events of these categories are the following:

a. $\mu\mu$ observed events (untagged)

Both muons penetrate the iron and hit the TOF counter. At least one muon reaches the outer chamber, having $P_t(\mu) > 1.5$ GeV. $P(\mu) < 0.5 * E_{beam}$ for each muon.

$E_{em} < 0.2*E_{beam}$, here E_{em} is the energy deposit of the event in the electromagnetic calorimeters.

b. $e\mu\mu$ observed events (single tagged)

The muon selection is the same as in case a, but $P(\mu) < 0.5*E_{beam}$, at least for one muon.

$E_{em} > 0.2*E_{beam}$. The electron is identified by checking drift tube tracks which must match with counter tracks found in the electromagnetic calorimeter, thus the $\mu\mu\gamma$ can be well seperated from $\mu\mu e$ events.

The total momentum unbalance cut

$$\Delta P = | \vec{P}_e+\vec{P}_{\mu 1}+\vec{P}_{\mu 2} | > 0.25*E_{beam}. \qquad (3)$$

is used for reducing the $\mu\mu\gamma$ background from electron identification ambiguity caused by a dead corner of vertex detector and the photon conversion to an e^+e^- pair.

c. $ee\mu$ and $ee\mu\mu$ observed events (double tagged)

At least one isolated muon penetrates the iron with $P_t(\mu) > 1.5$ GeV and hits a TOF counter.

$E_{em} > 0.2*E_{beam}$.

Two energetic tracks are found in the electromagnetic calorimeter, and at least one electron can be well identified.

The measurements were taken with the integrated luminosity for several $\sqrt{s}$ regions which are listed in Table 2. The number of $ee\mu\mu$ events accepted by Mark J detector with $\cos(\vartheta_\mu) < 0.87$ are shown in Table 3.

Table 2.

The data collected by Mark J detector and used in this analysis

$\sqrt{s}$ GeV	14	20-30	30-40	40-46.78
Lumi pb^{-1}	1.6	3.8	78.4	29.2

Table 3.

The number of $ee\mu\mu$ events accepted with $\cos(\vartheta_\mu) < 0.87$ for $14 < \sqrt{s} < 46.78$ GeV.

$\mu\mu$	$e\mu\mu$	$ee\mu$ & $ee\mu\mu$
3932	299	46

The four momentum transfer between incoming and outgoing electron is defined as

$$Q^2=|(P_{in}(e)-P_{out}(e))^2|. \qquad (4)$$

If an electron is scattered at large polar angle with respect to the beam axis and therefore is observed in the tagged detector, a certain momentum transfer to the off shell photon can be measured. The values of Q^2 for the three categories of $ee\mu\mu$ events are computed using Monte Carlo techniques including detector simulation.

Table 4.

Averaged Q^2 for $\mu\mu$, $e\mu\mu$ and $ee\mu\mu$ events at $\sqrt{s}$ = 35 and 44 GeV.

event type	averaged Q^2 GeV^2 $\sqrt{s}$ = 35 GeV	$\sqrt{s}$ = 44 GeV
$\mu\mu$	0.72	0.99
$e\mu\mu$	30.	42.
$ee\mu$+$ee\mu\mu$	92.	166.

We have studied the contamination from the processes of $ee \rightarrow \mu\mu\gamma$, $\tau\tau\gamma$, $ee\tau\tau$ using QED Monte Carlo events. The results show that these backgrounds for both $\mu\mu$ and $e\mu\mu$ observed events are at a negligible level.(see Table 5.) The background from $ee \rightarrow \mu\mu\gamma$, $\tau\tau\gamma$, $ee\tau\tau$ have been subtracted in the following distributions.

Table 5.

The contaminations from $ee \rightarrow \mu\mu\gamma$, $\tau\tau\gamma$, $ee\tau\tau$ processes

$\sqrt{s}$	35 GeV	44 GeV	Note
background	2.4 %	1.8 %	for untagged events
	1.1 %	0.8 %	for single tagged events

3 QED MONTE CARLO CALCULATION

The complete α^4 order QED calculation for the process of $ee \rightarrow ee\mu\mu$ includes 4 subsets of Feynman diagrams:

2 multiperipheral diagrams

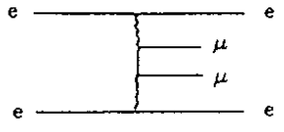

4 bremsstrahlung diagrams

4 conversion diagrams

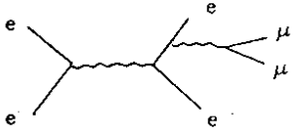

2 annihilation diagrams

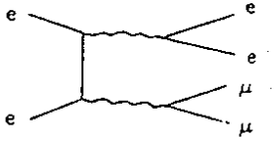

A complete α^4 order QED Monte Carlo program (B.D.K) [6] is used to generate $ee \rightarrow ee\mu\mu$ events with detector simulation. All interference terms between α^4 Feynman diagrams and lepton masses have been included in the calculation. The higher order radiative correction, estimated to be at the one percent level, is not included[7].

4 RESULTS

1. Total cross section

The observed cross section for ee $\longrightarrow$ ee$\mu\mu$ process as function of $\sqrt{s}$ by the Mark J detector is shown in Fig. 4 for untagged and tagged events respectively. A statistical error is given in the plot. The systematic error in the cross section measurement is about 4 % including errors of luminosity and detector efficiency.

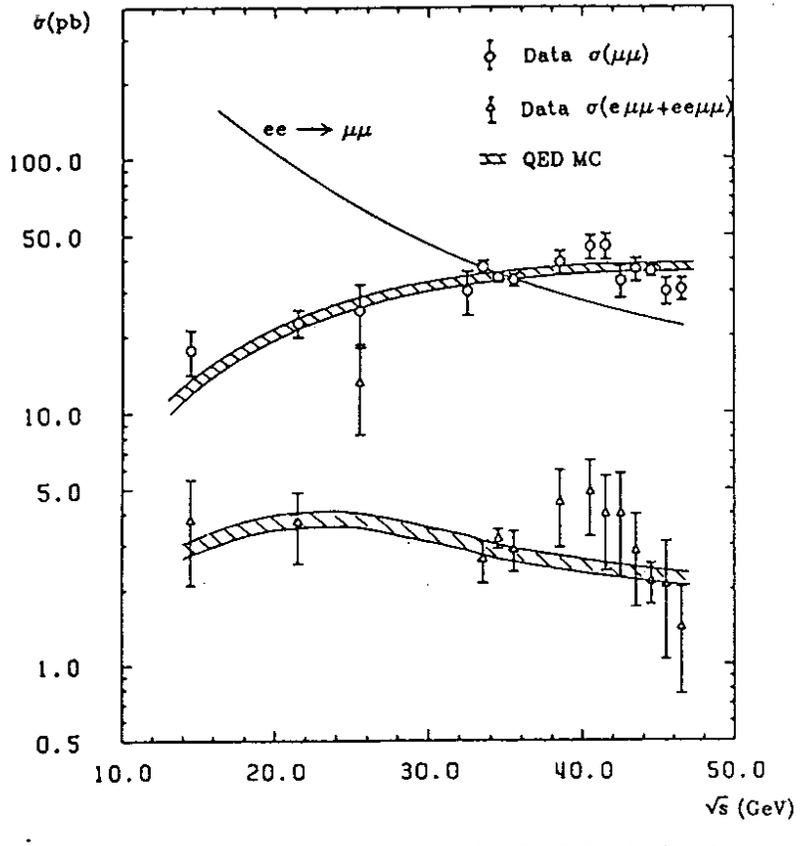

Fig. 4 The cross section in pb, observed in the Mark J detector, for ee $\longrightarrow$ ee$\mu\mu$ as function of $\sqrt{s}$.

$\sigma(\mu\mu)$ increases logarithmically as $\sqrt{s}$ increases from 14 GeV to 46.78 GeV. Our observations agree well with QED predictions. The number of events in the data and expected from the Monte Carlo calculation for $\sqrt{s}$ > 30 GeV are shown in Table 6.

Table 6.

The number of ee$\mu\mu$ events in the data and expected from the Monte Carlo for $\sqrt{s}$ > 30 GeV.

	$\mu\mu$	e$\mu\mu$	eeμ and ee$\mu\mu$
data	3671±61	283±17	43±7
MC	3834±31	256± 8	39±3

2. P_t behaviour

According to hard scattering models[8], the transverse momentum P_t of particle c in the deep-inelastic electromagnetic process

$$a + b \longrightarrow c + \text{anything} . \qquad (5)$$

would obey the power law P_t^{-B} ($B \sim 4$) for large P_t if a,b,c are point-like particles. The differential cross section as function of P_t, $d\sigma/dP_t^2$, provides a sensitive test of this model and is expected to be similar to the distribution of quark transverse momentum in two photon production via ee $\longrightarrow$ ee$q\bar{q}$ [4].

A bin-wise acceptance correction computed from QED Monte Carlo with detector response simulation, is made to the data. Fig. 6a) and 6b) show the observed $d\sigma/dP_t^2$ for 30 GeV < $\sqrt{s}$ < 40 GeV and for 40 GeV < $\sqrt{s}$ < 46.78 GeV respectively. P_t is the muon transverse momentum with respect to beam axis. The data fit well to a power law

$$d\sigma/dP_t^2 = A * P_t^{-B}. \qquad (6)$$

The best fit parameters for untagged events in the data, with $|\cos(\vartheta_\mu)|<0.87$ and $P_t^2 > 2$ GeV^2, are shown in Table 7 and Fig. 5 . The QED prediction for B vs. $\sqrt{s}$ is also plotted in Fig. 5 .

Table 7.

The best fit parameters A and B, for Data at averaged $\sqrt{s}$ = 34.7 and 44 GeV.

averaged $\sqrt{s}$ GeV		34.7	44.0
A	nb/GeV^2	0.53±0.05	0.45±0.07
B		4.67±0.12	4.47±0.15

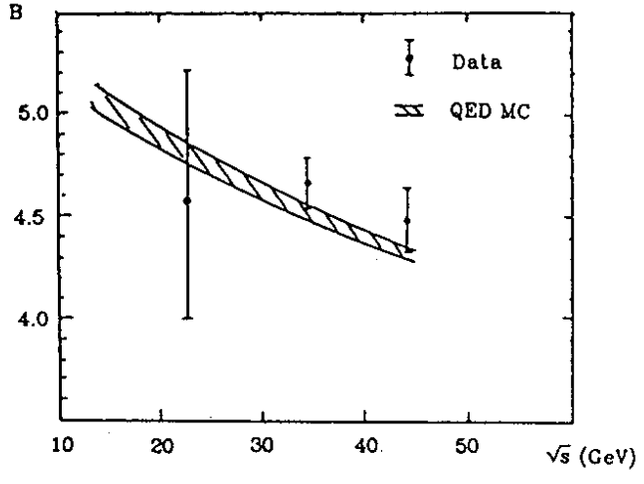

Fig. 5 The best fit values of B to the power law of $d\sigma/dP_t^2 = A*P_t^{-B}$ for $\mu\mu$ observed events, here $|\cos(\vartheta_\mu)| < 0.87$ and $P_t^2 > 2$ GeV^2, vs. $\sqrt{s}$. P_t is the muon transverse momentum with respect to the beam axis.

The P_t behaviour of muons observed in the data is well explained by the α^4 QED calculation. B depends upon $\sqrt{s}$, approaches 4 from above, and is expected to be 4 in the limit of $S \to \infty$.

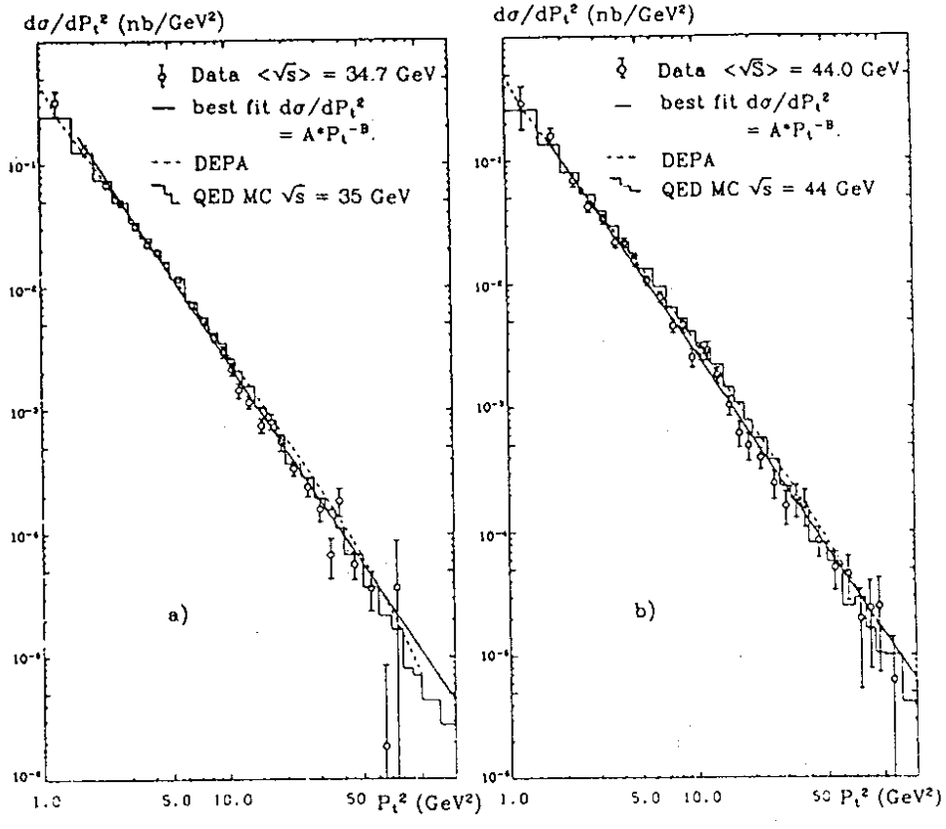

Fig. 6 Differential cross section as a function of the muon transverse momentum squared. The points are data. The solid curve is the best fit with the power law $d\sigma/dP_t^2 = A*P_t^{-B}$. The dotted curve is based upon the double equivalent photon approximation(DEPA). The histograms are α^4 QED Monte Carlo predictions. a) $40 > \sqrt{s} > 30$ GeV, b) $46.78 > \sqrt{s} > 40$ GeV.

In the untagged events the photons can be seen as quasi-real. The DEPA(Double Equivalent Photon Approximation)[9] is thus valid. As one sees from Fig. 6, DEPA describes the data very well at both $\sqrt{s}$ = 35 and 44 GeV in the untagged events as expected.

3. Acoplanarity and acollinearity distributions

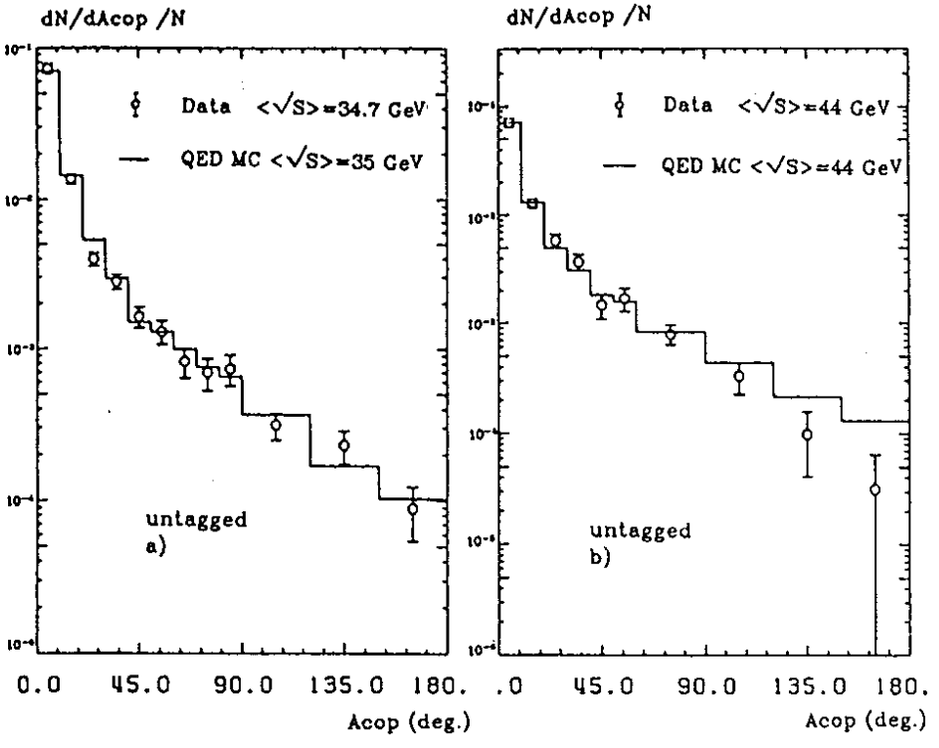

Fig. 7 The acoplanarity for two muons in the two photon reaction for the untagged case. a) $40 > \sqrt{s} > 30$ GeV, b) $46.78 > \sqrt{s} > 40$ GeV.

Acoplanarity and acollinearity are defined as

$$\text{Acop} = 180° - \Phi; \quad \text{Acol} = 180° - \xi. \qquad (7)$$

where Φ is the angle between two muon momentum projections in the plane perpendicular to the beam axis and ξ is the angle between the directions of two muon momenta. Figs. 7, 8 and 9 show the acoplanarity and acollinearity distribution of muon pairs in the two photon process for $\sqrt{s} < 40$ and $\sqrt{s} > 40$ GeV.

In the untagged case, the electrons remain in the beam pipe. The transverse momentum is well balanced and the two muons tend to be coplanar with the beam axis. This explains the peak at Acop=0. Because of bremsstrahlung feature of quasi-real photons, the longitudinal momentum of the electrons do not have to be balanced and the two muons are not collinear.

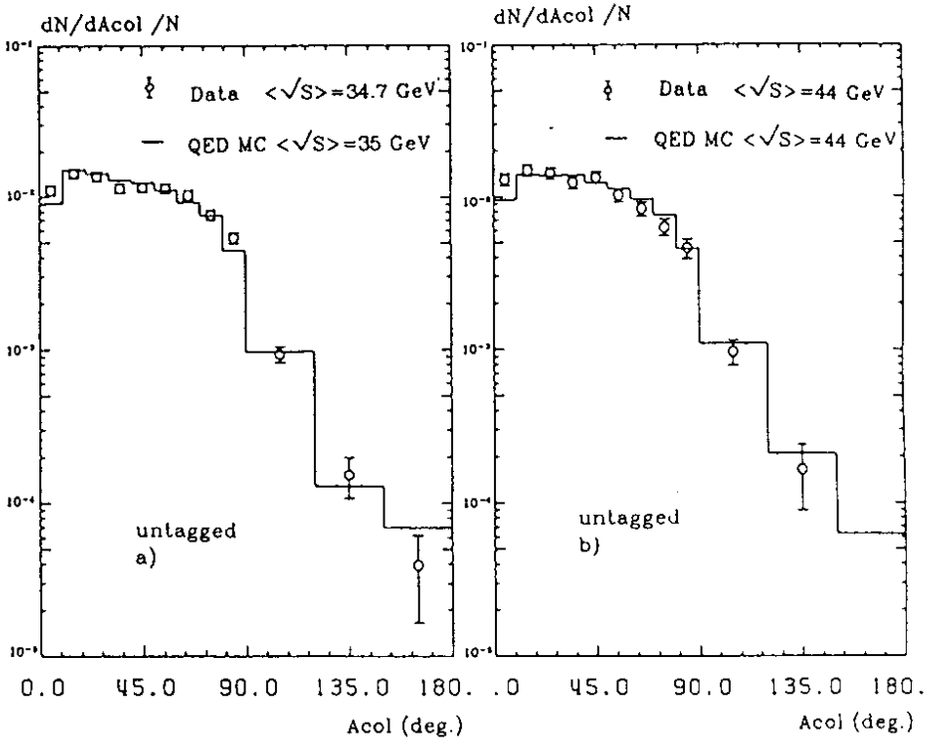

Fig. 8 The acollinearity for two muons in the two photon reaction for the untagged case. a) $40 > \sqrt{s} > 30$ GeV, b) $46.78 > \sqrt{s} > 40$ GeV.

In the tagged case, electrons are observed at large scattering angles $\vartheta_e > 12$ deg . The two muons are no longer coplanar and become even more acollinear.

The acoplanarity and acollinearity distributions are well described by QED Monte Carlo calculations in both untagged and tagged cases.

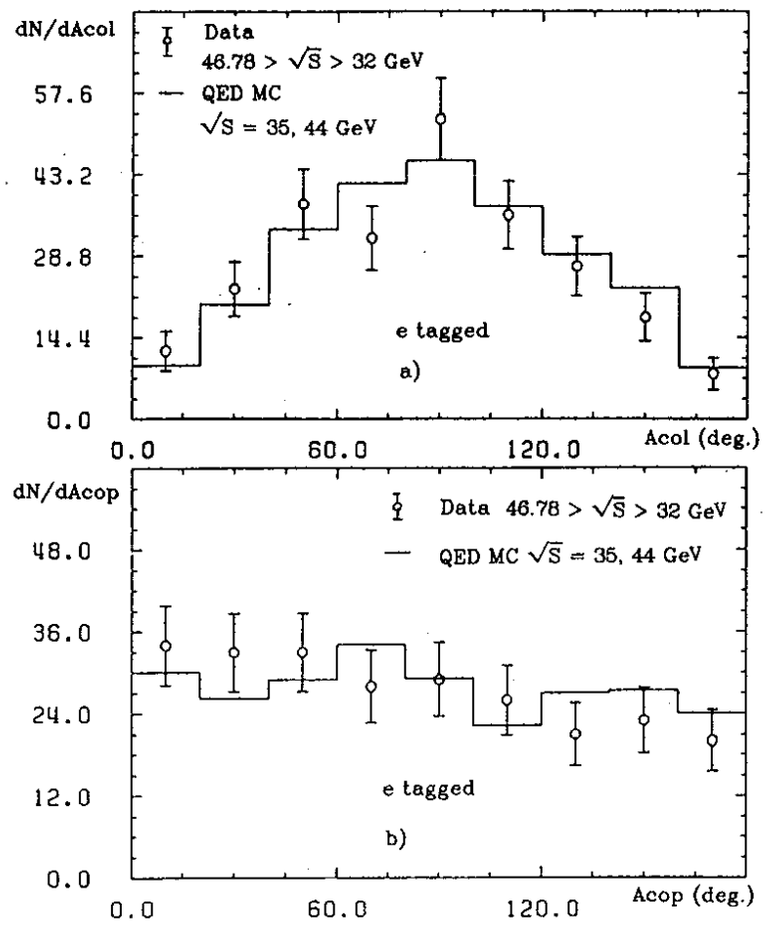

Fig. 9 a) the acollinearity and b) the acoplanarity for two muons in the two photon reaction for the single tagged case, $46.78 > \sqrt{s} > 30$ GeV.

4. Q^2 and x distribution

In the tagged events, the mass of the off shell photon can be calculated by means of the outgoing electron energy E_{out} and its scattering angle ϑ_e :

$$Q^2 = (P_{in}(e) - P_{out}(e))^2 = 2*E_{in}(e)*E_{out}(e)*(1-\cos(\vartheta_e)). \quad (8)$$

where $E_{in}(e) = E_{beam}$. The scaling variable

$$x = Q^2 / (Q^2 + M_{\mu\mu}^2) \quad (9)$$

can also be calculated since the mass of the muon pair is well measured. The Q^2 and x distribution of the data for both single and double tagged events again agree well with Monte Carlo predictions (see Fig. 10). No excess is observed in the range of $x > 0.9$ from our data in comparison with the complete α^4 QED Monte Carlo calculation which includes the bremsstrahlung diagrams.

Fig. 10 a)

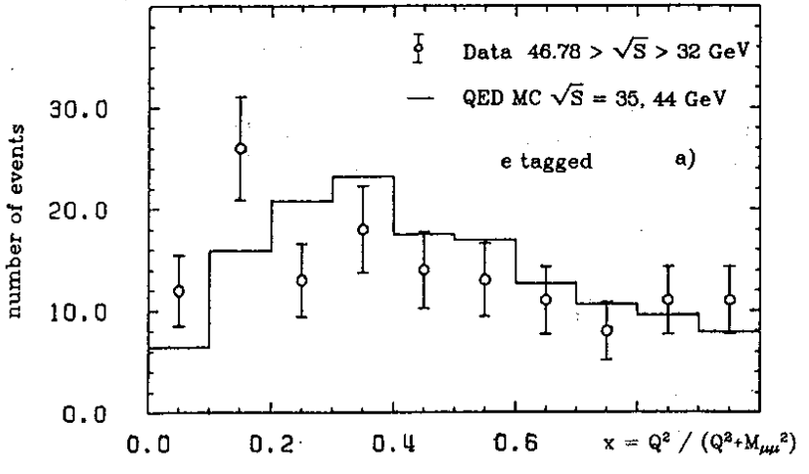

Fig. 10 a) x plot for single tagged events;

PLUTO and PEP-9 has observed an excess in their $M_{\mu\mu}$ or x distributions [2] in comparison with the QED calculation with only two multiperipheral Feynman diagrams. This excess can be well explained by the contribution of the bremsstrahlung Feynman diagrams which have been included in our studies.

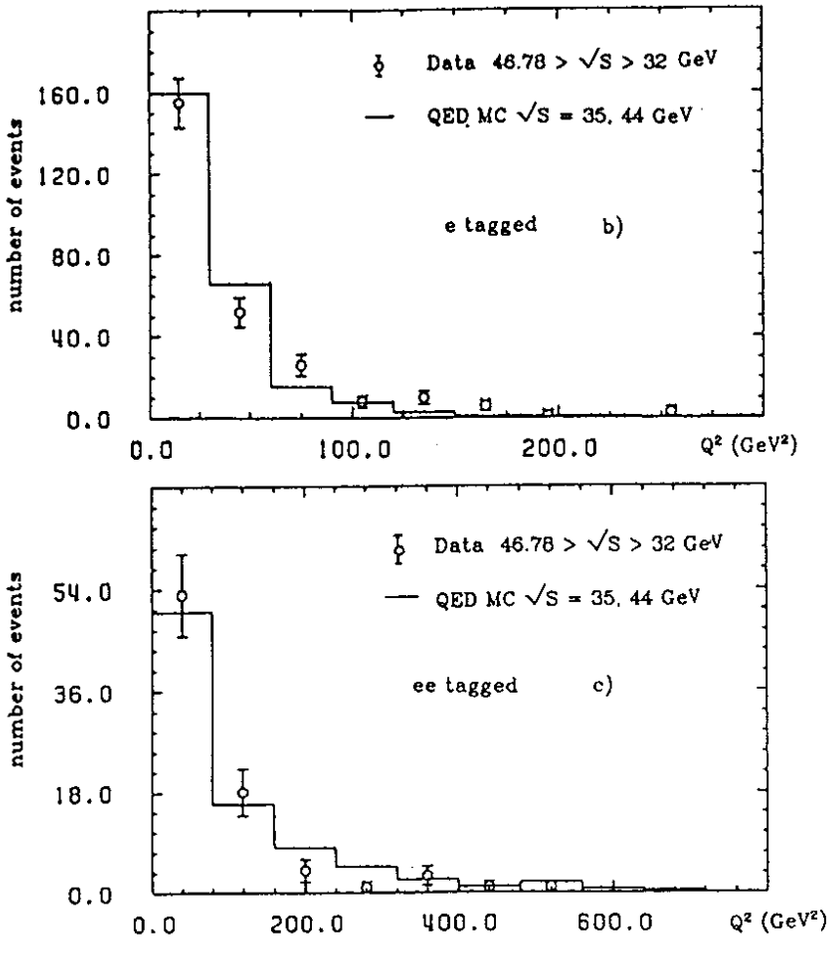

Fig. 10 b) and c) Q^2 for single and double tagged events separately, at $46.78 > \sqrt{s} > 30$ GeV.

5. Invariant mass of muon pairs

Fig. 11 shows ths invariant mass distribution of the muon pairs in two photon production for the untagged case. The resolution of the invariant mass measured by Mark J detector, which is computed from muon pairs in one photon production, is about 15% for P_μ = 7 GeV/c. No indication for a new state with C = +1 decaying into $\mu\mu$ is seen in the range of $M_{\mu\mu} < 10$ GeV/c^2 from our invariant mass distribution of muon pairs.

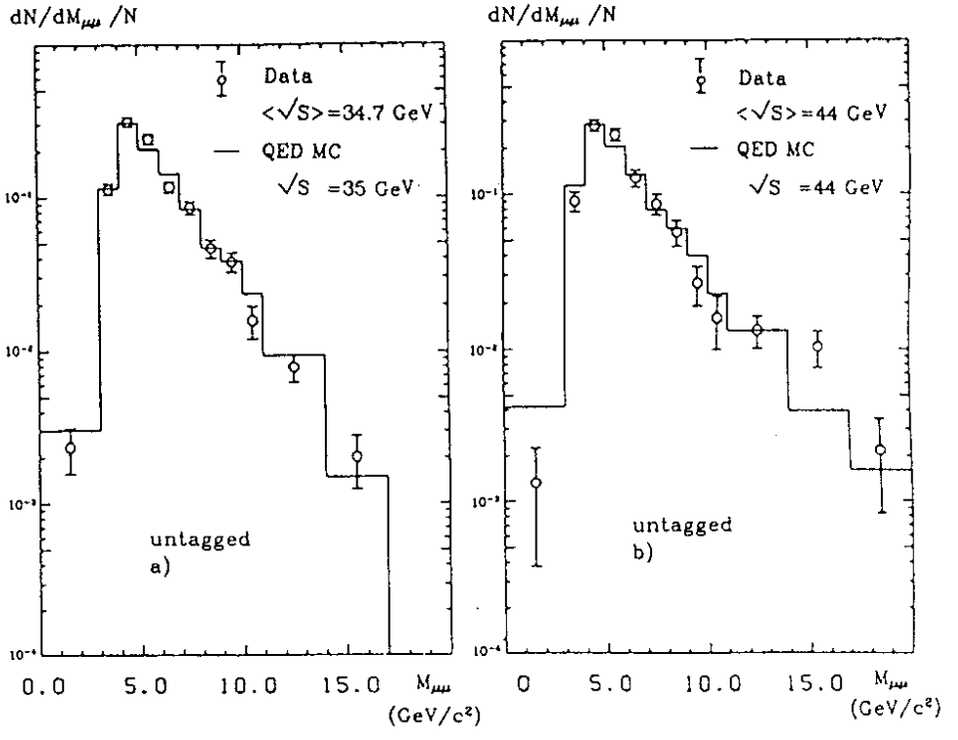

Fig. 11 The invariant mass distribution of the muon pairs in the two photon reaction for the untagged case, a) $40 > \sqrt{s} > 30$ GeV, b) $46.78 > \sqrt{s} > 40$ GeV.

The invariant mass of muon pair for single tagged events in the data is well described by the complete α^4 QED prediction (see Fig. 12).

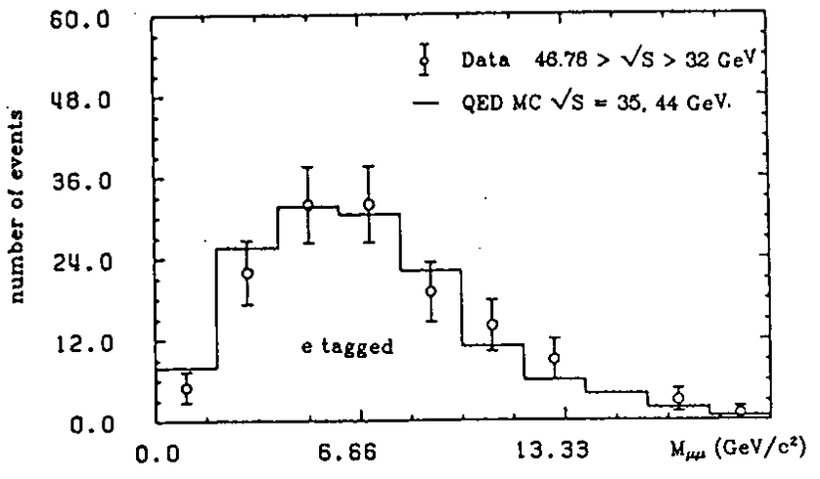

Fig. 12 The invariant mass distribution of muon pairs in the two photon reaction for the single tagged case, 46.78 > $\sqrt{s}$ > 30 GeV.

6. Charge Asymmetry of muons

According to QED, muon pair production is dominated by the

multiperipheral diagram

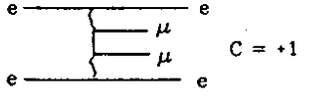

and has a 1 % contribution

from the bremsstrahlung diagram

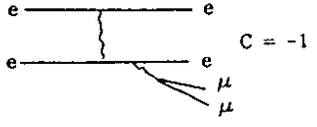

A small charge asymmetry in muons could be caused by the interference between these two kinds of diagrams with +1 and -1 charge parity.

The charge asymmetry is defined as following:

$$\text{Asym} = \frac{(N(\mu^-,f) + N(\mu^+,b) - N(\mu^-,b) - N(\mu^+,f))}{(N(\mu^-,f) + N(\mu^+,b) + N(\mu^-,b) + N(\mu^+,f))} \quad (10)$$

where $N(\mu^-,f)$ is number of μ^- in forward direction (i.e. direction of the incoming e^-) and so on.

Recently, F.A.Berends, P.H.Deverveldt and R.Kleiss (B.D.K) have calculated this asymmetry using their α^4 complete QED Monte Carlo generator, and found[6],

$$\text{Asym} = (0.81 \pm 0.05) \% \quad (11)$$

with

E_{beam} = 17 GeV, $W_{min}(\mu\mu)^2$ = 1 GeV²
$E(e^+)$ > 3.6 GeV, $8.02 < \vartheta(e^+) < 20.64°$
$0 < \vartheta(e^-) < 5°$, $|\cos(\vartheta_\mu)| < 0.92$

The muon charge asymmetry observed from the data at 30 GeV < $\sqrt{s}$ < 46.78 GeV and the MC at $\sqrt{s}$ = 35 and 44 GeV, with $|\cos(\vartheta_\mu)| < 0.80$ are listed in Table 8. and 9. for both the untagged and tagged cases, respectively.

Table 8.

The charge asymmetry of muons in $\mu\mu$ observed events for Data and QED MC.

	Asym⁺ % positive polarity	Asym⁻ % negative polarity	Avr Asym = (Asym⁺+Asym⁻)/2 %
Data	17.6±1.6	-18.3±1.7	-0.4±1.2
MC	19.8±0.7	-20.5±0.7	-0.4±0.5

Table 9.

The charge asymmetry of muons in $e\mu\mu$ observed events for Data and QED MC.

	$Asym^+$ % positive polarity	$Asym^-$ % negative polarity	Avr Asym = $(Asym^+ + Asym^-)/2$ %
Data	15.0±5.8	4.6±6.8	9.8±4.5
MC	7.0±3.0	-6.1±3.0	0.5±2.1

where $Asym^+$ is the asymmetry of charged muons measured with positive magnetic polarity and so on. The apparent non-zero values of $Asym^+$ and $Asym^-$ are mainly due to the acceptance for muons. Approximately, equal luminosity has been collected with each kind of magnetic polarity, therefore the polarity effect is canceled in the averaged Asym = $(Asym^+ + Asym^-)/2$.

As seen in the above table, no significant asymmetry is obtained in untagged events in agreement with the QED Monte Carlo. Our measured asymmetry for single tagged events is found to be (9.8±4.5) %, which is 2σ far away from QED Monte Carlo prediction of (0.5±2.1) %

We have used the cut for Acop > 25 deg and $P_t(\mu\mu)$ / E_{beam} > 0.1 to separate some tagged events with a small scattering angle for the electron from our untagged events, in which the electron is scattered inside the beam pipe with $5° < \vartheta(e) < 10°$ and therefore is not detected. From these additional tagged events with $5° < \vartheta(e) < 10°$ and averaged Q^2 = 5.3 GeV^2 (8.0 GeV^2) at $\sqrt{s}$ = 35 GeV (44 GeV), we found

Asym = (-1.8±4.7) % in data
Asym = (-0.4 ±1.9) % in MC

CELLO has found a positive asymmetry[2] in both $ee\mu\mu$ and eeee final states but has not give the values measured. The averaged Q^2 in their single tagged events is 9.5 GeV^2

95% of the tagged events in PLUTO data[2] have averaged Q^2 = 0.5 or 5 GeV^2. They found

Asym = (1±3) % in data
Asym = (2 ±1) % in MC

From the above results, there is some indication that this asymmetry exists only for large Q^2 values in $ee\mu\mu$ production and not in the small Q^2 region.

7. Searching for exotic particles

We have searched for an excess in the region of large y over QED prediction. Here we use a variable

$$y = \text{Min}\,(M(l^+l^-))/E_{beam}. \qquad (12)$$

where Min ($M(l^+l^-)$) is the smallest of $M(\mu\mu)$ and M(ee).

The cut criteria made in the CELLO[10], Mark J and JADE[10]experiments are shown in Table 10.

Table 10.

The cut criteria for large angle $ee\mu\mu$ event selection used in CELLO, Mark J and JADE data analysis

	CELLO	Mark J	JADE
Lumi pb^{-1}	32.6	113.0	94.0
$\lvert\cos(\vartheta_e)\rvert$	< 0.92	< 0.94	< 0.955
P_e	> 1.0 GeV	> 0.2*E_{beam}	> $E_{beam}/3$
$\lvert\cos(\vartheta\mu)\rvert$	< 0.92	< 0.87	<0.966
$P(\mu)$	> 1.0 GeV	> 1.5 GeV	> 1 GeV
$M(l^+l^-)$	> 1 GeV	> 1 GeV	-

9 events with four final leptons($ee\mu\mu$) observed are selected after cuts, while the QED Monte Carlo predicts 6.4. The y plot is shown in Fig. 13a). 2 events are found for y above 0.4, and this is in good agreement

with the QED expectation of 1.2 . No excess in the y > 0.4 region is found in our data.

The y plots from CELLO and JADE are also shown as a comparison (see Fig 13b) and c)). In JADE's measurement, the data agree with α^4 QED Monte Carlo predictions in whole region of 1 > y > 0 for both eeee and ee$\mu\mu$ final states. As seen from CELLO's plot, among their 13 ee$\mu\mu$ observed events, 7 are found in y > 0.4 region, whereas 1.2 is expected. They found an excess for y above 0.4 with the probability of 0.2% due to a statistical fluctuation of the QED expectation. Our data shows no such abnormality as observed by CELLO even though our integrated luminosity is a factor of 3.5 times larger than theirs.

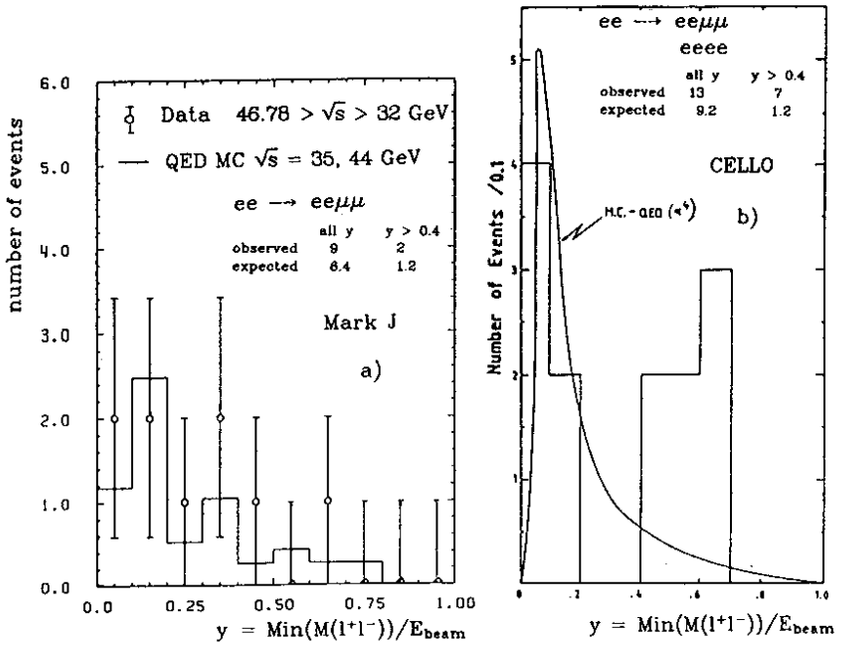

Fig. 13 The y = Min(M(l^+l^-))/E_{beam}distribution of four lepton final states in which four leptons are observed, a) Mark J, b) CELLO.

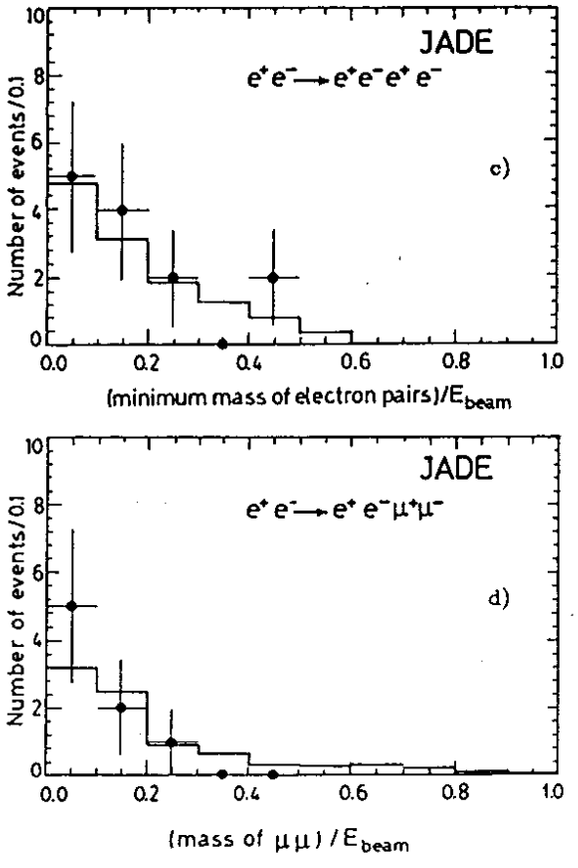

Fig. 13 The y = Min(M(l^+l^-))/E_{beam}distribution of four lepton final states in which four leptons are observed, c), d) JADE.

5 CONCLUSION

1. Our study shows that the complete α^4 order QED calculation (B.D.K.) describe the data of two phton muon pair production very well over a wide range of $\sqrt{s}$, (14 GeV to 46.78 GeV), and averaged Q^2 = 0.7 GeV^2 to 166 GeV^2

2. $d\sigma/dP_t^2$ shows a power law behaviour, $A^*P_t^{-B}$, and B = 4.5±0.2 at $\sqrt{s}$ = 44 GeV.

3. The charge asymmetry of muons for single tagged events is found to be 9.8±4.5 with averaged Q^2 = 30 GeV^2 at $\sqrt{s}$ = 35 GeV and Q^2 = 42 GeV^2 at $\sqrt{s}$= 44 GeV, while QED Monte Carlo predicts 0.5±2.1 .

4. No abnormality is observed in the number of events with all 4-leptons ($ee\mu\mu$) observed in the region of $Min(M(l^+l^-)/E_{beam} > 0.4$ in contradiction to CELLO's observation.

Acknowledgments

I greatly appreciate Prof. Samuel C.C. Ting for his invaluable guidance and encouragement in my study at DESY for a period of four and half years. I would like to thank Profs. A. Böhm, M. Chen and R. Rau for their helpful suggestions and discussions. I also wish to thank Profs. M. Chen, R. Rau and G. Weber and Dr. J. Burger for their careful reading of this paper.

I thank the directors of DESY, Prof. V. Soergel and Prof. P. Söeding for their hospitality.

References

1. J.Builey et al., Nucl. Phys. B150(1979)1.
R.S.Van Dyck et al., Phys. Rev. Lett. 38(1979)310.
K. Von Klitzing et al., Phys. Rev. Lett. 45(1980)494.
H.J. Behrend et al., Z. Phys. C16(1983)301.
W.Bartel et al., Phys. Lett. 108B(1982)160 and DESY 83-035
B.Adeva et al., Phys. Rev. Lett. 48(1982)1701.
Ch. Berger et al., Phys. Lett. 99B(1981)292.
R. Brandelik et al., Phys. Lett. 117B(1982)365.
E. Fernandez et al., Phys. Rev. Lett. 50(1983)1238

2. B. Adeva et al., Phys. Rev. Lett. 48(1982)721.
H.-J. Behrend et al., Phys. Lett. 126B(1983)384.
Ch. Berger et al., DESY 84-098 (1984).
M.P. Cain et al., Phys. Lett. 147B(1984)232.

3. M. Pohl, 5th Int. Workshop on Photon-Photon Collision, Aachen, April 1983; DESY 83-047(1983).

4. H. Spitzer, DESY 80-043 (1980);
W. Bartel et al., Phys. Lett. 107B(1981)163;
R. Brandelik et al., Phys. Lett. 107B(1981)290;
H.J. Behrend et al., Phys. Lett. 123B (1983) 127
W.Bartel et al., Z.Phys. C24 (1984) 231
M.Althoff et al., Phys. Lett. 138B (1984) 219
Ch. Berger et al., Phys. lett. 142B (1984) 111

5. D.P.Barber et al.,Phys. Rev. Lett. 43(1979)1915.
D.P.Barber et al.,Phys. Rep. 63(1980)337
B. Adeva et al., Phys. Rev. Lett. 48(1982)1701.
B. Adeva et al., Phys. Rep. 109(1984)131

6. F.A.Berends et al., Nucl. Phys. B253(1985)441.
R. Kleiss et al, Nucl. Phys. B241(1984)61.
For other QED calculations also see:
R. Bhattacharya et al., Phys. Rev. D15(1977)3267.
J. Smith et al., Phys. Rev. D15(1977)3280;
J.A.M. Vermaseren et al., Phys. Rev. D19(1979)137.
J.A.M. Vermaseren et al., Nucl. Phys. B229(1983)347.
F.A. Berends et al., Z. Physik C22(1984)239.

7. F.A.Berends et al., Nucl. Phys. B253(1985)421.
W.L.Van Neerven et al., Nucl. Phys. B238(1984)73.
Amiens 1980, G. Cochard and P. Kessler Edts, Lecture Notes in Physics 134(1980)35.

8. S.M. Berman, J.D. Bjorken, J.B.kogut, Phys. Rev. D4(1971)3388;
S.J. Brodsky et al., Phys. Rev. Lett. 41(1978)672;
K.Kajantie and P. raito, Nucl. Phys. B159(1979)528.

9. C. Carimalo et al., Phys. Rev. D20(1979)1057;
A. Coureau, CAL 82/19 (1982).
J.H. Field, Nucl. Phys. B168(1980)477;
Ch. Berger and J.H. Field, Nucl. Phys. B187(1981)585.

10. H.-J. Behrend et al., DESY 84/103 (1984);
JADE Internal report (unpublished).